Initial Results of X-ray Imaging and Energy Spectrum Measurements of Hot Electron Plasmas in RT-1

Haruhiko SAITOH, Yoshihisa YANO, Tatsunori MIZUSHIMA, Junji MORIKAWA and Zensho YOSHIDA

Graduate School of Frontier Sciences, The University of Tokyo, 5-1-5 Kashiwanoha, Kashiwa, Chiba 277-8561, Japan

(Received 19 August 2009 / Accepted 28 September 2009)

To acquire spatial profiles and energy spectra of hot electrons in ECH plasmas, we installed a soft x-ray pinhole camera in RT-1. In this publication, we compare the results of an initial experiment using a mechanically supported dipole field coil with the measurements of plasma pressure for different microwave frequencies. The results indicate that the coil support structure was the major loss channel for the high temperature electrons.

Keywords: internal coil device, magnetospheric configuration, high-beta plasma, x-ray camera

DOI: 10.1585/pfr.4.050

Plasma experiments in artificial magnetospheres, generated by levitated superconducting magnets [1, 2], began with the goals of understanding the physics of flowing plasmas [3, 4] and realizing dipole fusion reactors as D-D and D-^{3}He power sources [5]. Stable confinement of plasmas with local β values of up to 40 % has been achieved in Ring Trap 1 (RT-1) [1, 6] using coil levitation and compensation of the geomagnetic error fields [7]. In RT-1, plasmas are created by electron cyclotron resonance heating (ECH) with 2.45 and 8.2 GHz microwaves, and the magnetically-trapped high energy electrons thus generated constitute the main component of the plasma pressure. Measurements of x-ray emission by Si(Li) detectors confirm the presence of high temperature electrons in the plasma, but detailed spatial profiles of the hot electrons have not been investigated previously. The pressure profiles provide important parameters for studying the equilibrium and stability properties of high β plasmas in the dipole field configuration. Thus, we installed a soft x-ray pinhole camera [8] in RT-1. The initial results from this camera are reported here.

Figure 1 shows the top view of RT-1 [6] and the schematic of the soft x-ray camera. For this experiment, we mechanically supported the dipole field coil with a current of 250 kA at the equator of the chamber because of a problem with an emergency coil catcher system. The levitation coil operated at 26 kA, which is 90 % of the rated value for the coil levitation. The magnetic separatrix generated by the combination of the dipole field and levitation coils was at $r = 95$ cm on the $z = 0$ cm plane. The working gas was helium. Transmitting and receiving antennas of a 4 mm microwave interferometer were positioned at the top and bottom ports at $r = 62$ cm. The plasma pressures were measured by four magnetic flux loops. The x-ray camera

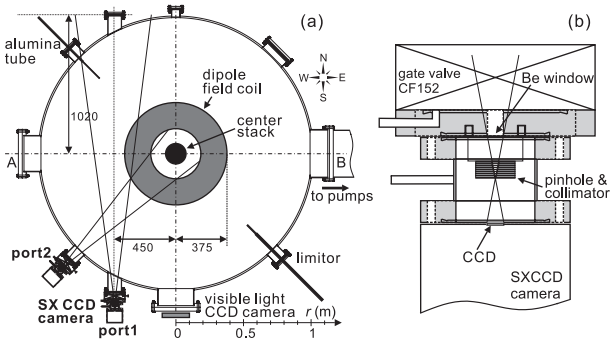

Fig. 1 (a) Top view of RT-1 including vacuum chamber and x-ray camera ports. (b) Schematic of soft x-ray camera.

was set on either (1) the south tangential or (2) the southwest ports at $z = 0$ cm (Fig. 1 (a)). The camera consisted of a 1024×1024 pixel soft x-ray CCD image sensor with a size of 13×13 mm, a 0.5 mm-thick stainless-steel plate with a 0.5 mm-diamiter pinhole, a 12 mm-thick lead collimator [8], and a 0.3 mm-thick beryllium filter. The apparatus measures a photon energy range from 2 keV to 10 keV, and the energy resolution of the CCD at 5 keV is 140 eV.

There were two electron populations with different temperatures in the ECH plasmas in RT-1. The hot electrons had an energy range of 1-10 keV. Their bremsstrahlung was detected using the Si(Li) photodiodes and the x-ray CCD camera. Langmuir probe measurements indicated that the cold electrons, generated primarily by collisions with high energy electrons and ionizations of neutrals, had temperatures of around 10 eV. The ratio of the two populations was controlled by varying the plasma production conditions. Figure 2 shows the line averaged electron density and diamagnetic signals $\Delta\Phi$ for various neutral gas pressures $p_{\rm gas}$ and RF powers $P_{\rm rf}$ of

author's e-mail: saito@ppl.k.u-tokyo.ac.jp

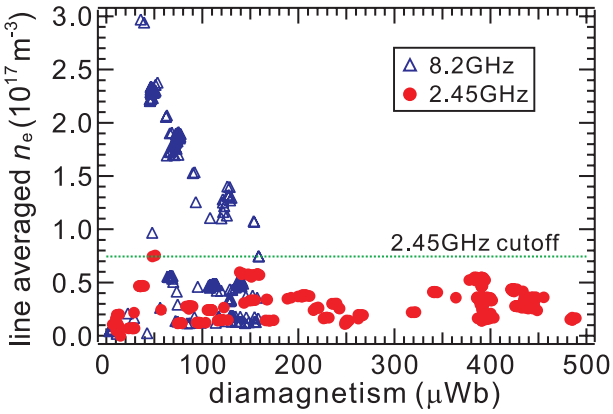

Fig. 2 Diamagnetic signals and line averaged electron densities in variations of rf powers 1-20 kW and neutral gas pressure 1-50 mPa for 2.45 and 8.2 GHz RF.

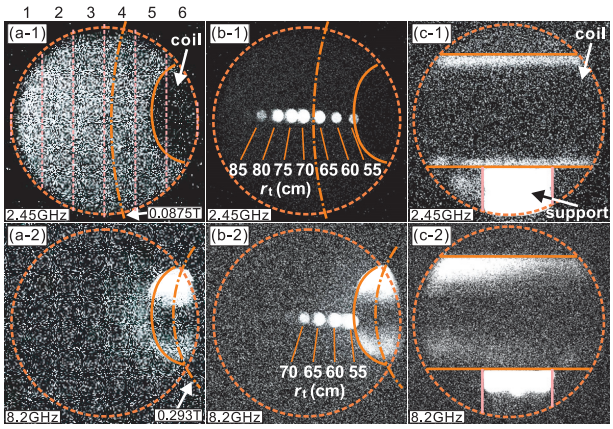

Fig. 3 Soft x-ray images observed from (a) port 1, (b) port 1 with insertion of target tube at different radial positions, and (c) port 2, generated by (1) 2.45 and (2) 8.2 GHz RF.

the 2.45 and 8.2 GHz RF sources. Although the plasma pressure was relatively low in the present experiment due to the mechanically supported coil, we found distinctly different plasma parameters for the different RF frequencies. 2.45 GHz RF caused a drastic increase of the high temperature electron component by reducing p_{gas} below approximately 10 mPa, resulting in an increase in the plasma pressure. $\Delta\Phi = 0.5$ mWb corresponds to the maximum local β value of 6 % [7]. In contrast, plasmas generated by the 8.2 GHz source exhibited relatively small diamagnetic signals. We note that ECH discharge cleaning is especially effective for 8.2 GHz ECH plasmas, and drastic improvements in the plasma parameters have been realized in recent experiments with the levitated coil in operation.

Figure 3 shows typical soft x-ray images of ECH plasmas generated by 2.45 and 8.2 GHz RF waves. The camera was positioned at port 1 for (a) and (b), and at port 2 for (c). For Fig. 3 (b), a 15 mm-diameter alumina tube was inserted into the plasma from the northwest port as a target for x-ray

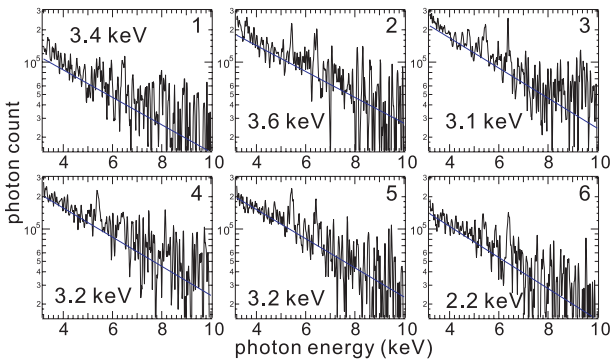

Fig. 4 Energy spectra of x-rays from plasma measured by CCD camera in photon counting mode. Image area was divided into 6 regions as shown in Fig. 3 (a-1).

bremsstrahlung and for detection of high energy electrons. We observed bremsstrahlung only at the end of the tube that is hemispherical in shape. The images were acquired from multiple exposures taken while varying the position of the tube end r_t from 100 to 55 cm. The field of view of the CCD camera (dotted line), the edge of the dipole field coil (solid line), and the ECR layers (chain lines) at the AB cross section of Fig. 1 (a) are plotted. The ECR layer of 2.45 GHz with $B = 0.0875$ T did not intersect the superconducting coil, while that of 8.2 GHz with $B = 0.293$ T did intersect the coil case. For 2.45 GHz discharges, x-rays were observed over the entire field of view except for the superconducting coil. Hot electrons were detected by the alumina tube when $r_t \leq 85$ cm. When 8.2 GHz RF was applied, the x-ray emitting region was localized near the coil, and emissions from the alumina tube were observed when $r_t \leq 70$ cm. Bremsstrahlung produced by energetic electrons colliding with the coil were also detected, indicating that some of the hot electrons were lost on the metal surface before filling the confinement region. These observations are consistent with the relatively small $\Delta\Phi$ for 8.2 GHz given in Fig. 2. The vertical asymmetry of the x-ray emitting region is probably because the RF was injected from a waveguide located at the top of the chamber and the magnetic surfaces were vertically asymmetric. For both the RF used, the major loss channel for hot electrons was the support structure of the coil, from where we observed strong bremsstrahlung x-ray in Fig. 3 (c).

The CCD camera has a 16-bit dynamic range photon counting capability [8]. Figure 4 shows x-ray energy spectra obtained by the pulse height analysis of the CCD signals under conditions of small photon flux ($P_{rf} = 3$ kW). We used Cr and Fe Kα Lines (5.41 and 6.40 keV, respectively) for the energy calibration, and estimated the photon count using the transmittance of the Be window and the quantum efficiency of the CCD. The electron temperature in the main confinement region (area 1-5 in Fig. 3 (a-1)) was $T_e = 3.4 \pm 0.3$ keV, which roughly agrees with the Si(Li) photodiode measurements that found $T_e = 3.8$ keV

for the same plasma shots. In the present experiment with the mechanically supported superconducting coil, we did not observe clear spatial dependence in T_e.

This work was supported by JSPS (19340170).

[1] Z. Yoshida *et al.*, Plasma Fusion Res. **1**, 008 (2006).
[2] D.T. Garnier *et al.*, Phys. Plasmas **13**, 056111 (2006).
[3] S.M. Mahajan and Z. Yoshida, Phys. Rev. Lett. **81**, 4863 (1998).
[4] Z. Yoshida and S.M. Mahajan, Phys. Rev. Lett. **88**, 095001 (2002).
[5] A. Hasegawa, Com. Plasma Phys. Cnt. Fusion **1**, 147 (1987).
[6] Y. Ogawa *et al.*, Plasma Fusion Res. **4**, 020 (2009).
[7] Y. Yano *et al.*, Plasma Fusion Res. **4**, 039 (2009).
[8] Y. Liang *et al.*, Rev. Sci. Instrum. **72**, 717 (2001).